

See discussions, stats, and author profiles for this publication at: <https://www.researchgate.net/publication/231632194>

Solid-State and Flexible Dye-Sensitized TiO₂ Solar Cells: a Study by Electrochemical Impedance Spectroscopy

ARTICLE *in* PROCEEDINGS OF SPIE - THE INTERNATIONAL SOCIETY FOR OPTICAL ENGINEERING · MAY 2002

Impact Factor: 0.2 · DOI: 10.1021/jp014456u

CITATIONS

247

READS

195

3 AUTHORS, INCLUDING:



Ana Flávia Nogueira

University of Campinas

97 PUBLICATIONS 2,715 CITATIONS

SEE PROFILE



Marco Aurelio De Paoli

University of Campinas

275 PUBLICATIONS 6,584 CITATIONS

SEE PROFILE

Solid-State and Flexible Dye-Sensitized TiO₂ Solar Cells: a Study by Electrochemical Impedance Spectroscopy

Claudia Longo, A. F. Nogueira, and Marco-A. De Paoli*

Laboratório de Polímeros Condutores e Reciclagem, Instituto de Química, Unicamp, C.Postal 6154, 13083–970 Campinas, SP, Brazil

H. Cachet

Laboratoire de Physique des Liquides et Electrochimie, UPR15–CNRS, Tour 22-E5 4, Place Jussieu, 75252 Paris cedex 05, France

Received: December 10, 2001; In Final Form: March 7, 2002

Dye-sensitized TiO₂ solar cells were assembled using rigid or flexible transparent electrodes (a conductive film deposited on glass or on poly(ethylene terephthalate) as substrates and a polymer electrolyte based on I₃[−]/I[−] and poly(epichlorohydrin-co-ethylene oxide)). The cells were characterized by current–potential curves and electrochemical impedance spectroscopy under different light intensities. Under 100 mW cm^{−2} illumination, the rigid cell exhibited an open circuit potential V_{OC} = 0.82 V, a short-circuit photocurrent I_{SC} = 2.2 mA cm^{−2}, and an efficiency η = 1%; for the flexible cell, V_{OC} = 0.72 V, I_{SC} = 0.40 mA cm^{−2}, and η = 0.1%. Under illumination, impedance spectra of the cells exhibited three semicircles. In the dark, both systems presented very high impedance. The differences in the efficiency and the impedance spectra of both cells were compared and discussed.

Introduction

Regenerative dye-sensitized photoelectrochemical cells have been under investigation for the past decade. The low production costs and good efficiency for energy conversion, reaching 10% in some cases, make such devices a promising alternative for the development of a new generation of solar cells.^{1–3} Their energy conversion working principle is based upon the injection of electrons from a photoexcited state of the sensitizer into the conduction band of the semiconductor. A charge mediator, i.e., a suitable redox couple, must be added to the electrolyte for rereducing the oxidized dye. The mediator also needs to be renewed in the counter-electrode, making the photoelectrochemical cell regenerative.^{1–3}

In general, these devices are sandwich-type electrochemical cells, where the photoelectrode consists of a film of dye-sensitized nanocrystalline TiO₂ and the counter-electrode is a thin Pt film, both deposited on the surface of a transparent electrode, e.g., glass coated with a conductive film of fluorine-doped tin oxide (FTO) or indium tin oxide (ITO). The electrolyte is usually an organic solvent containing the redox couple I₃[−]/I[−].^{1–3} Thus, the configuration of these cells requires a perfect sealing in order to avoid leakage and evaporation of the solvent, contamination with impurities, etc.^{4–10}

Several attempts have been made to substitute the liquid electrolyte in the TiO₂/dye cells. Different results can be found in the literature. However, comparison is difficult since the active area of the cells, not always revealed, can be different. In general, cells assembled with electrolytes consisting of the same redox system in a polymer gel medium^{5–14} or in molten salts¹⁵ presented better efficiency than cells assembled with hole-conductor materials (iodine free electrolytes).^{4,16–18}

In our Laboratory, we have assembled a solid-state version of the regenerative dye-sensitized TiO₂ solar cell using a polymer electrolyte based on the elastomer poly(epichlorohydrin-co-ethylene oxide), poly (EO-EPI), from Daiso Co. Ltd., Osaka.^{7–10} This polymer electrolyte makes the assembly of the cell much easier and eliminates several problems related to the use of liquid electrolytes. In a previous work, we also demonstrate that this polymer electrolyte achieves excellent penetration into the pores of the TiO₂ film.⁸ However, the use of a dry polymer electrolyte reduces the efficiency of the cell in comparison to those with liquid electrolytes. The best efficiency for energy conversion (η) that we have obtained for a solid-state TiO₂/dye cell (with an active area of 1 cm²) was η = 2.6% under 10 mW cm^{−2} (η = 1.6% under 100 mW cm^{−2}).^{8,9} Thus, such devices have a potential application in conditions of low illumination, for instance in the shadows of a forest.

Presently, we are searching for a lower cost and broader applicability for TiO₂/dye photocells, using the polymer electrolyte and also flexible electrodes.¹⁰ Flexible electrodes, like the films of poly(ethylene terephthalate) coated with tin-doped indium oxide (ITO–PET), presents lower cost and some technological advantages, considering aspects such as the fragility as well as the form and shape limitations of glass electrodes. For these reasons, its use has increased for assembling photoelectrochemical devices based on TiO₂/dye^{19,20} or on conjugated polymers systems.^{21,22}

The major problem in development of flexible TiO₂/dye solar cells by replacement of a glass electrode by a flexible one consists of manufacturing the TiO₂ porous electrode. Usually, porous TiO₂ electrodes are prepared by depositing a film of TiO₂ particles on the surface of a transparent glass electrode, followed by sintering at 450–500 °C.^{1,2} This thermal treatment eliminates organic residues (commonly used in the TiO₂

* To whom correspondence should be addressed. E-mail: mdepaoli@iqm.unicamp.br.

suspension) and induces electrical contact between the particles and the substrate.^{1,23} Since PET-ITO degrades at such temperatures, alternative processes were applied to prepare the porous photoelectrode.^{10,19,20}

This contribution reports on the preparation and characterization of solid-state TiO₂-dye solar cells assembled with a polymer electrolyte and rigid (glass-FTO) or flexible (PET-ITO) electrodes, and their investigation by Electrochemical Impedance Spectroscopy (EIS).

Experimental Section

Photoelectrochemical cells were assembled using glass-FTO electrodes prepared by Spray Pyrolysis²⁴ (15 $\Omega\Box$), or flexible PET-ITO electrodes (Innovative Sputtering Technology, 60 $\Omega\Box$) as substrates for the photoelectrode and counter-electrode.

Counter-electrodes (CE) were obtained by sputter depositing a thin Pt film onto glass-FTO or PET-ITO. For preparation of photoelectrodes, a small aliquot of TiO₂ suspension (Ti nan-oxide-T, *Solaronix*) was spread onto the rigid or the flexible electrodes using a glass rod with an adhesive tape as spacer ($\sim 42\ \mu\text{m}$). The glass-FTO | TiO₂ electrode was heated at 450 °C for 30 min in an oven, while the PET-ITO | TiO₂ electrode was heated at 130 °C for 4 h in an oven placed inside a drybox filled with argon. The electrodes were cooled to $\sim 80\ ^\circ\text{C}$ in a desiccator, immersed during 16 h in a $1.5 \times 10^{-4}\ \text{mol L}^{-1}$ solution of the sensitizer dye cis-bis(isothiocyanato)bis(2,2'-bipyridyl-4,4'-dicarboxylato)-ruthenium(II), (Ruthenium-535, *Solaronix*) in absolute ethanol, rinsed with ethanol and then dried.

Afterward, a film of the polymer electrolyte was deposited onto the sensitized electrodes by casting, using a solution of 0.3 g of poly(EO-EPI, 84:16) (Daiso), 27 mg of NaI, 3 mg of LiI, and 7 mg of I₂ in 25 mL of acetone. The conductivity of such a polymer electrolyte depends on the concentration ratio of oxygen in the ethylene oxide repeating units and the cation, $\alpha = [\text{O}]_{\text{EO}}/[\{\text{Na}^+ + \text{Li}^+\}]$. For this electrolyte, $\alpha = 25$, which gives an ionic conductivity of $1.5 \times 10^{-5}\ \text{S cm}^{-1}$ for $[\text{H}_2\text{O}] < 1\ \text{ppm}$ and $2.0 \times 10^{-4}\ \text{S cm}^{-1}$ at 86% relative humidity, according to previous measurements.²⁵

The assembly of the solid solar cells was done by pressing the rigid or the flexible CE against the sensitized electrodes coated with the solid electrolyte. An adhesive tape (42 μm) was placed between the two electrodes, to control electrolyte film thickness and to avoid short-circuiting of the cell. The active area of the cells was 1.0 cm².

The efficiency of the devices was investigated on an optical bench having an Oriol Xe (Hg) 250 W lamp. Water and cut off filters were used to avoid IR and UV radiation and light intensity was varied using neutral density filters. I_{SC} and I - V measurements under illumination were recorded using variable resistance and a digital multimeter, Minipa ET2500, coupled to a computer.

EIS measurements were performed with the Eco-Chimie Autolab PGSTAT 10 with FRA module. The device was connected in a two-electrode configuration: the sensitized porous electrode was connected as working electrode (the contact was in a naked FTO or ITO extremity) and the Pt CE was used as pseudo-reference (circuited with the counter-electrode). I - V curves were also obtained with this configuration and using linear sweep voltammetry at $0.5\ \text{mV s}^{-1}$. EIS spectra were obtained by applying sinusoidal perturbations of $\pm 10\ \text{mV}$ over the V_{OC} at frequencies from 10^{-2} to $10^5\ \text{Hz}$, in the dark and under illumination. EIS measurements were also done for a cell consisting of two Pt electrodes sandwiching a film of the polymer electrolyte and using an adhesive tape to control the

film thickness (configuration: glass-FTO | Pt || polymer electrolyte || Pt | FTO-glass). The EIS results were analyzed using Boukamp software.²⁶

The surface of the TiO₂ films deposited on glass-FTO or PET-ITO was also examined after the thermal treatment using a JEOL JSM 6340F High-Resolution Field Emission Scanning Electron Microscope.

Results and Discussion

Scanning Electron Microscopy revealed very similar morphology for the TiO₂ films deposited on both types of substrates. However, the film was more uniform and the particles were more compact on the surface of the PET-ITO | TiO₂ electrode than on the surface of the rigid electrode. The micrographs are available as Supporting Information, Figure 1 Sa and 1Sb.

The use of ITO-PET for developing dye-sensitized TiO₂ flexible electrodes has been previously discussed.^{10,19,20} In previous studies, we observed that the transparency and conductivity of the flexible electrode remain unchanged up to 145 °C.¹⁰ Also, dye attachment was higher when the PET-ITO | TiO₂ electrode was heated in dry conditions, probably because dye attachment on TiO₂ depends on reducing the water content at the oxide surface.²³ Thus, we performed the thermal treatment at 130 °C in a drybox and we have obtained reasonably mechanically stable TiO₂ films, which presented a good adsorption of the dye. Nevertheless, coloration and absorbance spectra confirmed that dye attachment was more effective for the glass electrode (fired at 450 °C). The compactness of the TiO₂ film and the presence of surfactant residues (from the suspension) may decrease the adsorption of the dye.

Current-Potential Curves for Solid-State Rigid or Flexible Dye-Sensitized TiO₂ Cells. The performance of the cells was characterized by measuring the variation of the short-circuit current with time and current-voltage curves under different incident light intensities over ten days. On the first and second days after assembling, both the cells exhibited identical open circuit potentials, $V_{\text{OC}} = 0.82\ \text{V}$, with short circuit currents of $2.2\ \text{mA cm}^{-2}$ for the rigid cell and $0.59\ \text{mA cm}^{-2}$ for the flexible one under $100\ \text{mW cm}^{-2}$ illumination. The photocurrent and photopotential of the flexible cell gradually decreased to $I_{\text{SC}} = 0.40\ \text{mA cm}^{-2}$ and $V_{\text{OC}} = 0.72\ \text{V}$ and then remained unchanged from the fourth to the tenth day after cell assembling. The performance of the cell assembled with glass-FTO electrodes did not change during this period.

Figure 1 shows the current-voltage characteristics of the rigid and the flexible cells determined one week after cell assembling. Similar results were obtained for I - V curves determined with the potentiostat and using variable resistances. The values for open circuit voltage V_{OC} , short-circuit current I_{SC} , fill factor ff , and overall conversion efficiency η , obtained from the curves for both cells, are shown in Table 1.

In general, the photocurrent exhibited for the flexible version of the solid-state TiO₂/dye photoelectrochemical cell was almost five times lower than that observed for the rigid cell, and the efficiency depended on the light intensity. Similar results were observed in previous studies where dye-sensitized solar cells were assembled with the same polymer electrolyte but using a different TiO₂ suspension.²⁷ For those cells, however, photocurrent and efficiency of the flexible cell was ten times smaller than that observed for the cell assembled with glass-FTO electrodes.²⁷ The main reason for the lower performance of the flexible cell must be the poor electronic contact between the TiO₂ nanoparticles and the ITO-PET substrate, as discussed later.

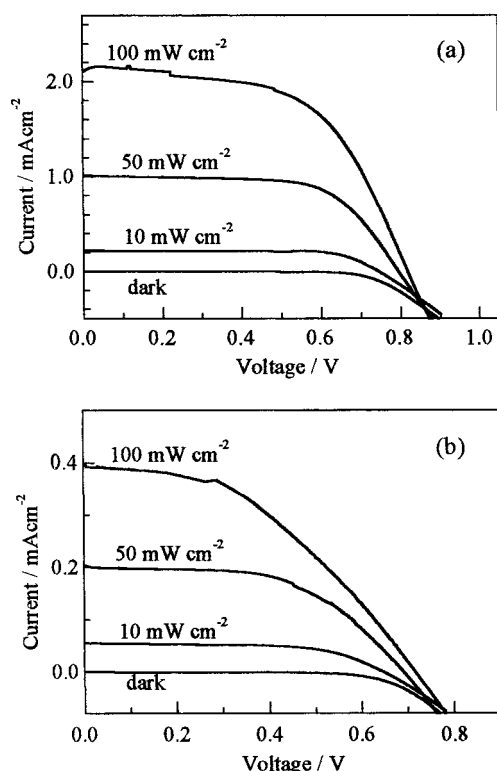


Figure 1. Current-potential curves obtained with different light intensities for solid-state dye-sensitized TiO₂ solar cells assembled with a polymer electrolyte and (a) glass-FTO and (b) PET-ITO electrodes.

TABLE 1: Parameters for TiO₂-dye Solar Cells Assembled with a Polymer Electrolyte and Electrodes of Glass-FTO (rigid cell) or PET-ITO (flexible cell)

cell	intensity/ mW cm ⁻²	I _{sc} ^a /mA cm ⁻²	V _{oc} ^b /V	ff ^c	η ^d /%
rigid	100	2.2	0.82	0.56	1.0
	50	1.0	0.81	0.65	1.0
	10	0.22	0.75	0.67	1.2
flexible	100	0.40	0.72	0.42	0.12
	50	0.20	0.69	0.54	0.15
	10	0.056	0.65	0.61	0.22

^a Photocurrent. ^b Open Circuit Potential. ^c Fill factor. ^d Efficiency.

The open circuit voltage of both flexible and rigid solar cells assembled with the polymer electrolyte were comparable to those reported for TiO₂-dye cells assembled with liquid electrolytes. This property has already been discussed in our previous studies.^{8,9} The high V_{oc} values were attributed to the basic nature of the copolymer, which could interact with the acid sites of the TiO₂ surface and suppress part of the dark current.⁹ It is interesting to note that both the cell employing flexible ITO-PET and the cell employing a glass substrate, exhibited almost the same V_{oc} values. This is a strong evidence supporting the suggestion that the cause of the high voltage output is associated to the polymer electrolyte, since the electrodes consisted of different materials.

Electrochemical Impedance Spectroscopy for Solid-State Dye-Sensitized TiO₂ Cells. Figures 2–4 show the EIS spectra obtained for the cells in the dark and under illumination, using a perturbation of ± 10 mV over the open circuit potential (Table 1 displays V_{oc} values under illumination; in the dark, V_{oc} corresponded to 0.23 V for the rigid cell and 0.070 V for the flexible one). Experimental data are represented by symbols while the solid lines correspond to the fit obtained with Boukamp software using the equivalent circuit shown in Figure 5. Parameters obtained by fitting the experimental spectra with

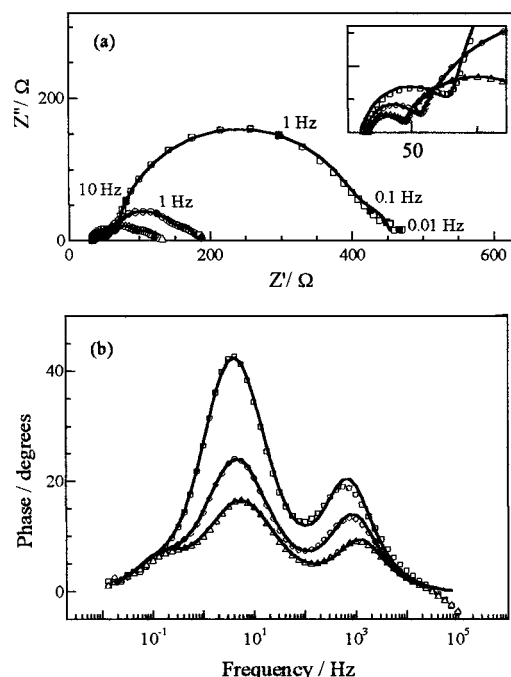


Figure 2. Nyquist (a) and Bode (b) diagrams of the impedance spectra obtained under illumination for a rigid TiO₂-dye solar cell assembled with a polymer electrolyte and glass-FTO electrodes. Insert in (a) is the magnification of the high-frequency region. Experimental data are represented by symbols and solid lines correspond to fits obtained with Boukamp software using the equivalent circuit in Figure 5. Light intensity: (□) 10 mW cm⁻²; (O) 50 mW cm⁻²; (Δ) 100 mW cm⁻².

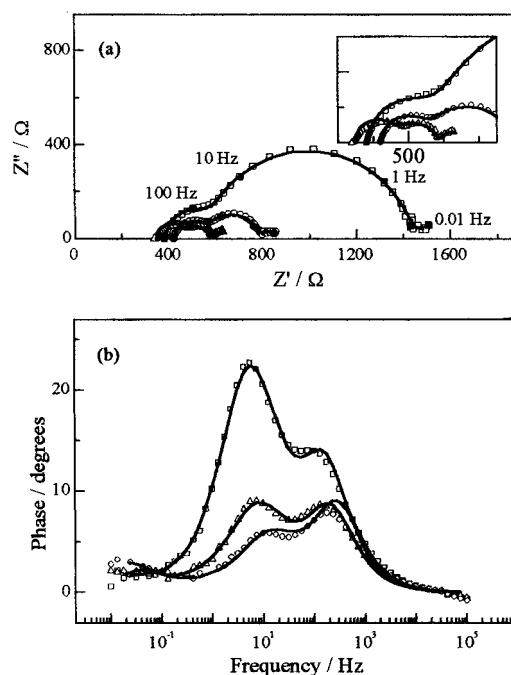


Figure 3. Nyquist (a) and Bode (b) diagrams of the impedance spectra obtained under illumination for a flexible solid-state TiO₂-dye solar cell assembled with a polymer electrolyte and PET-ITO electrodes. Insert in (a) is the magnification of the high-frequency region. Experimental data are represented by symbols and solid lines correspond to fit using the equivalent circuit in Figure 5. Light intensity: (□) 10 mW cm⁻²; (O) 50 mW cm⁻²; (Δ) 100 mW cm⁻².

this equivalent circuit, in the frequency ranging from 1.5×10^{-2} to 8.0×10^4 Hz are shown in Table 2.

The general behavior of the impedance spectra exhibited by the TiO₂-dye cells assembled with the polymer electrolyte poly

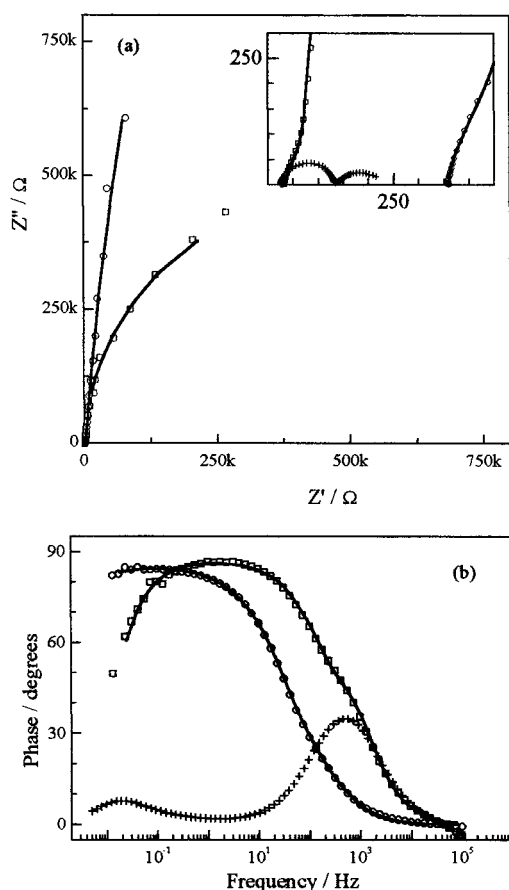


Figure 4. Nyquist (a) and Bode (b) diagrams of the impedance spectra obtained in the dark for TiO_2 -dye solar cells assembled with a polymer electrolyte and glass-FTO (\square) or flexible PET-ITO (\circ) electrodes and a cell consisting of the polymer electrolyte between two Pt electrodes ($+$). Insert in (a) is the magnification of the high-frequency region.

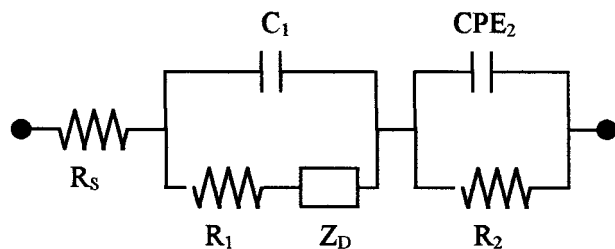


Figure 5. Equivalent circuit used to represent interfaces in solid-state solar cells consisting of substrate | TiO_2 -dye || poly(EO-EPI) + I_3^-/I^- || Pt | substrate, where substrate was a glass-FTO or a PET-ITO electrode.

(EO-EPI) was similar for cells prepared with different TiO_2 suspensions. Moreover, the impedance of the flexible cell is higher than that of the rigid one. The Nyquist diagram obtained for the rigid cell under illumination (Figure 2a) exhibited three semicircles. Under 10 mW cm^{-2} , however, the semicircle observed at low frequencies cannot be easily identified. For the flexible cell, three semicircles can also be identified in the spectra obtained under 50 and 100 mW cm^{-2} (Figure 3a). In the dark, both the cells presented high impedance and the time constants were not well defined (Figure 4). Probably, the high impedance exhibited by both cells in the dark can be related to the large resistance of the porous TiO_2 electrode. Figure 4 also shows the impedance spectrum obtained under the same experimental conditions ($\pm 10 \text{ mV}$ over the V_{OC} , in the dark) for the cell consisting of the polymer electrolyte between two Pt electrodes.

Comparison of the Bode diagrams obtained for the photoelectrochemical cells under illumination and the Pt || electrolyte || Pt cell (Figs. 2b, 3b, and 4b) revealed some correspondence at low and high frequencies. Thus, it can be inferred that the response at high frequency is related to the counter-electrode | electrolyte interface and the response at low frequency can be associated with the diffusion process of species in the polymer electrolyte. Considering this hypothesis, the equivalent circuit represented in Figure 5, $R_s [C_1 (R_1 O_1)] (R_2 Q_2)$, was used for fitting the impedance spectra obtained for both cells with Boukamp software.²⁶ The symbols R and C describe a resistance and a capacitance, respectively, O , which depends on the parameters Y_{o1} and B , accounts for a finite-length Warburg diffusion (Z_{Dif}) and Q is the symbol for the constant phase element, CPE (its parameters are Y_{o2} and n).

The impedance of the Warburg diffusion in a finite-length region of length l_e (which might be the thickness between the electrodes) can be expressed by eq 1, where $R_{\text{Dif}} = B/Y_{o1}$, $\tau = B^2 = l_e^2/D$ and D is the diffusion coefficient of the diffusing species.²⁸

$$Z_{\text{Dif}} = R_{\text{Dif}} \{ [\tanh(j\omega\tau)^{1/2}] / (j\omega\tau)^{1/2} \} \quad (1)$$

The CPE is a nonideal frequency dependent capacitance, a characteristic that can be associated with a distribution of relaxation times or with a nonuniform distribution of current due to material heterogeneity.^{26,28} Its admittance is expressed by eq 2, where n is a constant ranging from $0 \leq n \leq 1$.²⁶

$$Y = Y_{o2} (j\omega)^n \quad (2)$$

Association of the elements of an equivalent circuit with the interfaces of the system is not straightforward. Dye-sensitized photoelectrochemical cells are complex systems consisting of several interfaces, where different processes take place. In this study, EIS measurements were performed using a small perturbation over the open circuit potential. Thus, under illumination, a high electron accumulation must be expected in the cell because photoinjected electrons are not extracted at the electrode contact.^{29,30}

Considering the equivalent circuit in Figure 5, R_s would describe the series resistance and the elements with subscripts 1 and 2 are related to the contribution of the interfaces of counter-electrode | electrolyte and porous electrode | electrolyte, respectively. Diffusion related elements could also be considered for the photoelectrode | electrolyte interface. However, this did not improve the fit. Probably, the diffusion process acts mainly for the mediator reduction at the counter-electrode.

The impedance at high frequency, associated to the R_s element, was ca. 33Ω for the rigid cell and 380Ω for the flexible one (Table 2). Usually, the R_s element is associated with the series resistance of the electrolyte and electric contacts in an electrochemical cell. For such solar cells, the R_s component can account not only for resistance of the polymer electrolyte, but also for the resistance within the TiO_2 film. For the cell assembled with the glass-FTO electrode, the sintering procedure guaranteed a good electric contact between the TiO_2 particles in the porous photoelectrode. Thus, R_s must relate mainly to the polymer electrolyte. On the other hand, for the flexible cell, the high value observed for R_s may also include a contribution of the inherent resistance of the TiO_2 particle network. For cells assembled with the same polymer electrolyte but using another TiO_2 suspension, R_s was 40Ω for the cell assembled with glass electrodes and 480Ω for the flexible cell.²⁷

TABLE 2: Parameters Obtained by Fitting the Impedance Spectra of TiO₂-dye Solar Cells Assembled with a Polymer Electrolyte and Electrodes of Glass-FTO (rigid cell) or PET-ITO (flexible cell), Using the Equivalent Circuit R_s [C₁ (R₁ O)] (R₂ Q₂) (Figure 5) ^a

intensity/mW cm ⁻²	$\chi^2/(10^{-4})$	R _s /Ω	C ₁ /μF	R ₁ /Ω	O		R ₂ /Ω	Q ₂	
					Y ₀₁ /S	B/s ^{1/2}		Y ₀₂ /mF s ⁿ⁻¹	n
Rigid cell									
100	2.2	34	12	13	0.067	1.8	50	1.5	0.83
50	2.3	33	12	20	0.056	1.9	94	0.95	0.88
10	5.0	32	10	32	0.040	2.2	340	0.37	0.93
dark	4.4	32	10	33	0.003	1.3	9.5 × 10 ⁵	0.013	0.98
Flexible cell									
100	2.7	350	5.7	110	0.056	4.2	120	0.22	0.86
50	6.0	420	6.9	130	0.050	3.5	240	0.18	0.86
10	1.2	380	6.6	180	0.049	3.7	870	0.075	0.90
dark	0.8	360	5.8	92	0.004	5.6	1.4 × 10 ⁷	0.014	0.96

^a Fitting performed with the Boukamp software. The symbols R, C, O, and Q account for resistance, capacitance, finite-length Warburg diffusion (ZDif), and constant phase element, respectively.

The response observed at high frequency in the impedance spectra was characterized by a small semicircle in the Nyquist plots (Figs. 2a and 3a), almost independent of light intensity. This semicircle was associated with C₁ and R₁ elements (Table 2). Moreover, considering the similarity with the impedance spectrum of the Pt || electrolyte || Pt cell, this response can be associated with the capacitance and charge-transfer resistance at the Pt | electrolyte interface. In the equivalent circuit, suggested for fitting the spectra (Figure 5), this interface was represented by the sub-circuit on the left side (elements with subscript 1). This sub-circuit also accounts for the contribution of the diffusion of the electroactive species in the polymer electrolyte, associated with the low-frequency response. Such characteristics may be related to the low conductivity of the polymer electrolyte and the reduced mobility of I₃⁻ in such a medium. This effect was discussed in previous studies performed with the rigid cell using transient absorption spectroscopy.⁹

For both photoelectrochemical cells, the medium-frequency response, which exhibited strong dependence on light intensity, was associated with the R₂Q₂ elements. These elements can be correlated with the TiO₂ | electrolyte interface, where an accumulation of electrons and redox species is expected. Comparing the values obtained for both cells (Table 2) revealed that the flexible cell exhibits higher values for R₂ resistance and lower values for the C₂ capacitance (associated to Y₀₂ and n parameters) than the analogous components of the cell assembled with the glass-FTO electrode. Such differences may also result from the low sintering temperature applied to the flexible photoelectrode, which caused a poor electric contact between the TiO₂ particles in the film.

The rigid and the flexible dye-sensitized TiO₂ solar cells also presented other differences. Analyzing the parameters Y₀₁ and B, related to the finite-length diffusion (Table 2), revealed that the diffusion resistance R_{Dif} is higher for the flexible cell in comparison to the rigid one. In the dark, R_{Dif} was 430 Ω for the cell assembled with glass electrodes and 1.4 kΩ for the flexible cell. The diffusion resistance decreased with illumination, corresponding to 27 Ω and 75 Ω under 100 mW cm⁻² for the rigid and the flexible cells, respectively. The diffusion coefficient D, estimated from values in Table 2, also differed for both the cells. Considering that the diffusion length l_e is the thickness between the electrodes (thus corresponding to the thickness of the adhesive tape, 42 μm), D corresponded to 5 × 10⁻⁶ cm² s⁻¹ and 1 × 10⁻⁶ cm² s⁻¹, for the rigid and the flexible cells, respectively. From the impedance spectrum obtained for the Pt || electrolyte || Pt cell, with the same area and thickness, R_s = 25 Ω, R_{Dif} = 60 Ω, and D = 1 × 10⁻⁶ cm² s⁻¹. This

indicates that the diffusion coefficient was also affected by the thermal treatment of the semiconductor and/or by the type of substrate. On the other hand, these values are not so different from the diffusion coefficients estimated for I₃⁻ species in different media.^{31,32} For instance, the diffusion coefficient is 2.8 × 10⁻⁶ cm² s⁻¹ in the highly viscous solvent N-methyl oxazolidinone³¹ and 3.4 × 10⁻⁶ cm² s⁻¹ in acetonitrile in a TiO₂ membrane.³²

Other equivalent circuits could also fit the spectra. For instance, the experimental spectra could also be well adjusted using a circuit consisting of a series combination of a resistance and three parallel RC sub-circuits, i.e., R_s (R₁C₁) (R₂C₂) (R₃C₃), already used for fitting the spectra of dye-sensitized solar cells.³³ However, taking into account the low conductivity of the polymer electrolyte, as well as the impedance response obtained for the cell Pt || electrolyte || Pt, it seemed more reasonable to consider an element describing the diffusion process in the electrolyte.

The EIS technique was previously used by other authors to investigate dye-sensitized solar cells, however, different interpretations of the data were given.^{29,30,33} The impedance spectra obtained for dye-sensitized TiO₂ solar cells by Kang et al.³³ also exhibited three time constants, and were fitted with the equivalent circuit R_s (R₁C₁) (R₂C₂) (R₃C₃). They did not consider the contribution of the Pt | electrolyte interface; two of the three parallel RC circuits in series were attributed to the ITO | TiO₂ and TiO₂ | electrolyte interfaces, and the other RC element was used to represent the electron transport in the TiO₂ film (they rejected the use of a Warburg diffusion related element in their system).³³ Lagemaat et al.²⁹ also investigated dye-sensitized TiO₂ solar cells by EIS and other frequency resolved techniques: intensity-modulated photocurrent spectroscopy (IMPS) and intensity-modulated photovoltage spectroscopy. They found only two time constants in the impedance spectra, which were fitted with a R(RC)(RC) equivalent circuit. The high-frequency small semicircle was identified with the counter electrode, while the low-frequency large semicircle was associated to the photoelectrode, taking into account the charge-transfer process that occurs across the TiO₂ | redox electrolyte. In disagreement with Kang et al.,³³ they discarded the contribution of the FTO | TiO₂ interface in the impedance spectra, considering an ohmic contact in such interface.³³ Similar assumptions were also considered for interpretation of IMPS results.³⁴ The EIS data interpretation in this work was applied to both types of cells (rigid and flexible) with good agreement and better accounted for the existing interfaces in the cell.

Conclusions

Solid-state rigid and flexible regenerative dye-sensitized TiO₂ solar cells were assembled using a polymer electrolyte and glass-FTO or PET-ITO transparent electrodes as substrates. Under 100 mW cm⁻² illumination, the rigid cell exhibited an open circuit potential $V_{OC} = 0.82$ V, a short-circuit photocurrent $I_{SC} = 2.2$ mA cm⁻², and an efficiency $\eta = 1\%$; while for the flexible cell values of $V_{OC} = 0.72$ V, $I_{SC} = 0.4$ mA cm⁻², and $\eta = 0.1\%$ were obtained.

Electrochemical Impedance Spectroscopy was used to investigate the cells in the dark and under illumination. The general behavior of the spectra was similar for both cells, but the impedance of the flexible cell was higher than that of the rigid one. Three time constants could be identified in the spectra, which depended on the intensity of illumination. At high frequencies, the response associated with a small capacitance (~ 12 μ F cm⁻² for the rigid cell and 7 μ F cm⁻² for the flexible one), which was almost independent of illumination, was attributed to the interface between the Pt counter electrode and the electrolyte. The response at medium frequencies, related to a high capacitance that strongly depended on light intensity, was attributed to the TiO₂ | electrolyte, since an accumulation of electrons and redox species is expected at this interface under open circuit conditions. The response at low frequencies was associated with diffusion processes in the electrolyte, considering the lower mobility of the I_3^- species in the polymer electrolyte. This assumption was supported by the similarities of the response at low and high frequencies, as well as the impedance spectrum of a Pt || polymer electrolyte || Pt cell. Finally, the high R_S value obtained for the flexible cell, in comparison to the rigid one (approximately 380 Ω and 33 Ω , respectively), can be related to poor electrical contact between the particles in the TiO₂ network due to the low sintering temperature. Considering the high V_{OC} and the small I_{SC} , it can be inferred that the high R_S is responsible for the lower performance exhibited by the flexible cell. Despite the low efficiency exhibited by these regenerative solar cells, they show promise for use under low illumination conditions.

Acknowledgment. The authors thank FAPESP for financial support (96/09983-0) and fellowships (C.L. 00/03086-3 and A.F.N. 98/10567-6) and also acknowledge helpful suggestions made during discussions at Quantsol 2001, particularly from Dr. L. Peter. They are also indebted to Dr. M. C. Gonçalves for the FE-SEM measurements.

Supporting Information Available: Micrographs obtained by high-resolution FE-SEM of the surface of the TiO₂ films deposited on glass-FTO (Figure 1Sa) and PET-ITO (Figure 1Sb). This material is available free of charge via the Internet at <http://pubs.acs.org>.

References and Notes

- (1) Nazeeruddin, M. K.; Kay, A.; Rodicio, I.; Humphry-Baker, R.; Müller, E.; Liska, P.; Vlachopoulos, N.; Grätzel, M. *J. Am. Chem. Soc.* **1993**, *115*, 6382.
- (2) Hagfeldt, A.; Grätzel, M. *Chem. Rev.* **1995**, *95*, 49.
- (3) Pelet, S.; Moser, J. E.; Grätzel, M. *J. Phys. Chem. B* **2000**, *104*, 1791.
- (4) Bach, U.; Lupo, D.; Comte, P.; Moser, J.-E.; Weissörtel, F.; Salbeck, J.; Spreitzer, H.; Grätzel, M. *Nature* **1998**, *395*, 583.
- (5) Matsumoto, M.; Miyazaki, H.; Matsuihiro, K.; Kumashiro, Y.; Takaoka, Y. *Solid State Ionics* **1996**, *89*, 263.
- (6) Cao, F.; Oskam, G.; Searson, P. C. *J. Phys. Chem.* **1995**, *99*, 17071.
- (7) Nogueira, A. F.; De Paoli, M.-A. *Sol. Energy Mater. Sol. Cells* **2000**, *61*, 135.
- (8) Nogueira, A. F.; Durrant, J. R.; De Paoli, M.-A. *Adv. Mater.* **2001**, *13*, 826.
- (9) Nogueira, A. F.; De Paoli, M.-A.; Montanari, I.; Monkhouse, R.; Nelson, J.; Durrant, J. R. *J. Phys. Chem. B* **2001**, *105*, 7517.
- (10) De Paoli, M.-A.; Machado, D. A.; Nogueira, A. F.; Longo, C. *Electrochim. Acta* **2001**, *46*, 4243.
- (11) Tennakone, K.; Senadeera, G. K. R.; Perera, V. P. S.; Kottegoda, I. R. M.; De Silva, L. A. A. *Chem. Mater.* **1999**, *11*, 2474.
- (12) Stathatos, E.; Lianos, P.; Krontiras, C. *J. Phys. Chem. B* **2001**, *105*, 3486.
- (13) Ren, Y.; Zhang, Z.; Fang, S.; Yang, M.; Cai, S. *J. Appl. Electrochem.* **2001**, *31*, 445.
- (14) Kubo, W.; Murakoshi, K.; Kitamura, T.; Wada, Y.; Hanabusa, K.; Shirai, H.; Yanagida, S. *Chem. Lett.* **1998**, 1241.
- (15) Matsumoto, H.; Matsuda, T.; Tsuda, T.; Hagiwara, R.; Ito, Y.; Miyazaki, Y. *Chem. Lett.* **2001**, 26.
- (16) Murakoshi, K.; Kogure, R.; Wada, Y.; Yanagida, S. *Sol. Energy Mater. Sol. Cells* **1998**, *55*, 113.
- (17) Tennakone, K.; Senadeera, G. K. R.; De Silva, D. B. R. A.; Kottegoda, I. R. M. *Appl. Phys. Lett.* **2000**, *77*, 2367.
- (18) Gebeyehu, D.; Brabec, C. J.; Padinger, F.; Fromherz, T.; Spiekermann, S.; Vachopoulos, N.; Kienberger, F.; Schindler, H.; Sariciftci, N. S. *Synth. Met.* **2001**, *121*, 1549.
- (19) Pichot, F.; Ferrere, S.; Pitts, R. J.; Gregg, B. A. *J. Electrochem. Soc.* **1999**, *146*, 4324.
- (20) Sommeling, P. M.; Späth, M.; Kroon, J.; Kinderman, R.; van Roosmalen, J. *Proceedings of the 16th European Photovoltaic Solar Energy Conference and Exhibition*, Glasgow, May 1–5, 2000.
- (21) Gazotti, W. A.; Nogueira, A. F.; Girotto, E. M.; Gallazi, M. C.; De Paoli, M.-A. *Synth. Met.* **2000**, *108*, 151.
- (22) Brabec, C. J.; Sariciftci, N. S.; Hummelen, J. C. *Adv. Funct. Mater.* **2001**, *11*, 15.
- (23) Hagfeldt, A.; Didriksson, B.; Palmqvist, T.; Lindström, H.; Södergren, S.; Rensmo, H.; Lindquist, S.-E. *Sol. Energy Mater. Sol. Cells* **1994**, *31*, 481.
- (24) Cachet, H.; Zenia, F.; Froment, M. *J. Electrochem. Soc.* **1999**, *146*, 977.
- (25) Nogueira, A. F.; Spinacé, M. A.; Gazotti, W. A.; Girotto, E. M.; De Paoli, M.-A. *Solid State Ionics* **2001**, *140*, 327.
- (26) Boukamp, B. A. *EQUIVCRT, version 4.51*, University of Twente, The Netherlands, 1995.
- (27) Longo, C.; Nogueira, A. F.; Cachet, H.; De Paoli, M.-A. *Proceedings of the 46th SPIE Annual Meeting*; Vol. 4465, San Diego, CA, 2001; p 21.
- (28) Macdonald, J. R. in *Impedance Spectroscopy*; Macdonald, J. R., ed.; John Wiley: New York, 1987.
- (29) van de Lagemaat, J.; Park, N. G.; Frank, A. J. *J. Phys. Chem. B* **2000**, *104*, 2044.
- (30) Franco, G.; Gehring, J.; Peter, L. M.; Ponomarev, E. A.; Uhlendorf, I. *J. Phys. Chem. B* **1999**, *103*, 692.
- (31) Papageorgiou, N.; Grätzel, M.; Infelta, P. P. *Sol. Energy Mater. Sol. Cells* **1996**, *44*, 405.
- (32) Zebede, Z.; Lindquist, S. E. *Sol. Energy Mater. Sol. Cells* **1998**, *51*, 291.
- (33) Kang, T.-S.; Chun, K.-H.; Hong, J. S.; Moon, S.-H.; Kim, K.-J. *J. Electrochem. Soc.* **2000**, *147*, 3049.
- (34) Van der Zanden, B.; Goossens, A. *J. Phys. Chem. B* **2000**, *104*, 7171.